ChemComm

COMMUNICATION

Cite this: *Chem. Commun.*, 2024, **60**, 9360

Received 28th May 2024,
Accepted 22nd July 2024

DOI: 10.1039/d4cc02576h

rsc.li/chemcomm

A visible-light regulated luminescent switch based on a spiropyran-derived Pt(II) complex for advanced anti-counterfeiting materials†

Xin Lei,‡ Ying Jiang,‡ Qingguo Zeng, Yuncan Dou, Haokun Zhang, Jiatao Ni,
Yinuo Zhuo, Wei Wang, Yeye Ai* and Yongguang Li *

A dual optical switch regulated by visible light has been developed through an integrated strategy, including luminescent Pt(II) and photochromic spiropyran (SP) as a triplet-sensitizer and photo-regulator building block, respectively. An efficient Förster resonance energy transfer (FRET) process is achieved, along with apparent and emissive color changes under visible light irradiation and temperature stimuli, which was utilized to develop advanced anti-counterfeiting materials.

Multi-stimuli switches based on bionics are developed as smart materials that respond to the surrounding environmental changes, including light, electricity, heat, mechanical pressure, and other perturbations.[1–4] Particularly, photo-controlled molecular switches with the excellent characteristics of non-contact remote control, non-invasiveness and waste-free nature can provide accurate spatiotemporal control and maintain the microenvironment invariable.[5–7] Due to their high sensitivity and fast responsiveness, photo-controlled switches have a broad application potential in the fields of optical communication and optoelectronic devices, chemical and biological sensors, pollution monitoring, military medical treatment, as well as data security storage.[8–16]

Spiropyran (SP) presents an ancient and important class of phototropic molecular switches and is attributed to the photochemical heterolysis of spiro C–O bonds, leading to the planarization of the two originally orthogonal heterocycles, resulting in an increase in the extent of π-conjugation in the merocyanine (MC) structure, accompanied by optical property changes.[17–19] The reversible isomerization between SP and MC can be realized by alternating ultraviolet and visible light irradiation.[20,21] Fast photo-responsiveness, high thermal stability, and low preparation cost make SP popular in a variety of applications, including sunglass lenses, optical recording, biological probes, chemical sensors, pollutant detection, drug delivery and release materials, optical devices, and anti-counterfeiting materials.[10,18,22–26] Although SP has been shown to possess excellent photochromic properties, it usually requires high-energy ultraviolet irradiation. The repeated light irradiation will cause photooxidation degradation, reduce its fatigue resistance and stability, and limit its application as an optical material.

Triplet-sensitized photochromism (TSP) and the photon upconversion strategy are effective methods to improve the stability and fatigue resistance of SP in the photochromic process.[17,27] Based on the TSP mechanism, the dissociation energy of C–O bonds can be effectively reduced to obtain visible-light-controlled molecular switches.[28] The function can be realized by integrating with metal complexes. Among the multifarious transition metal complexes, Pt(II) complexes own a d^8 electronic structure and a planar quadrilateral configuration.[29,30] Their optical properties can be adjusted by tailoring the structures of the ligands at the molecular level and controlling the packing behaviors at the assembly level.[31–33] The heavy metal involving spin–orbit coupling is beneficial to promote the intersystem crossing of excited electrons from the singlet to triplet excited state, harvesting phosphorescent emission with high quantum yield.[34,35] By introducing a Pt–C metal bond, the splitting energy of the d–d orbital can be raised, which would inhibit the non-radiative transition and further enhance the luminescence performance.[35] The planar geometry makes the Pt(II) coordinated complexes tend to form various aggregates through metal–metal and π–π stacking interactions, leading to electron distribution changes and variable apparent and luminescent colors.[36,37] Due to their high phosphorescence yield, large Stokes shift, and long lifetime, phosphorescent Pt(II) complexes are extensively explored as optical devices and chemical and biological sensors.[38–41]

Herein, an integrated strategy is adopted to prepare a visible-light-controlled TSP molecular switch (**Pt-SP-Ph**; Scheme 1). A coordinated Pt(II) moiety is introduced as a triplet sensitizer,

---

College of Material, Chemistry and Chemical Engineering, Key Laboratory of Organosilicon Chemistry and Material Technology Ministry of Education, Hangzhou Normal University, Hangzhou 311121, P. R. China. E-mail: aiyeye@hznu.edu.cn, yongguangli@hznu.edu.cn

† Electronic supplementary information (ESI) available. See DOI: https://doi.org/10.1039/d4cc02576h

‡ The authors contributed equally to this work.

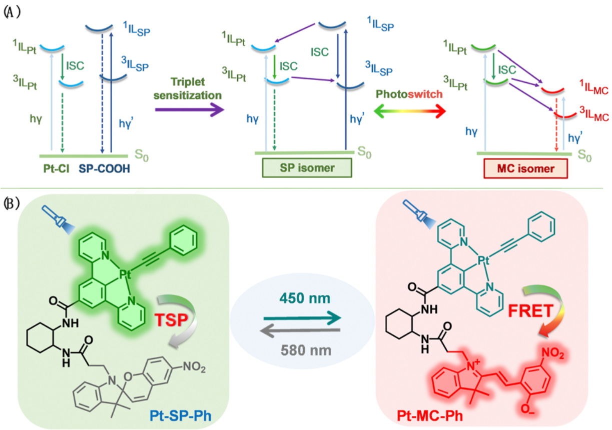

Scheme 1 (A) Illustration of the mechanism of the visible-light regulated molecular switch by TSP and (B) the design of photo-reversible FRET switch of **Pt-SP-Ph**.

so that the **Pt-SP-Ph** isomerization process from **Pt-SP-Ph** to **Pt-MC-Ph** can be achieved under lower-energy visible light irradiation. Under the alternating stimuli of visible light (λ_0 = 450 nm and λ_1 = 580 nm), the switching between colorless SP and the purple MC state with higher fatigue resistance and stability can be achieved. The modification of an auxiliary phenylacetylene ligand on the Pt(II) moiety not only improves the solubility but also enhances the optical properties. Importantly, the coordinated Pt(II) moiety with green emission has been designed and utilized because of the good overlap of its emission spectrum and the absorption spectrum of the MC moiety. To ensure efficient FRET, we designed the switch using cyclohexanediamine as the linkage to bridge the Pt(II) chromophore and SP photoisomer, serving as the donor and acceptor, respectively. This design minimizes their separation and facilitates an effective FRET system, thereby enhancing the deep red emission of **Pt-MC-Ph**. Based on the dynamic regulation of the optical switch *via* light and temperature, the switch has been applied as an optical anti-counterfeiting and photoerasable ink and as a temperature sensor.

Pt-SP-Ph shows good solubility in THF solution and its optical and photochromic properties in the solution state were firstly studied. The UV-vis spectrum displays high-energy, intense absorption bands at 268–362 nm assigned to the intraligand (IL) [π → π*] transitions of the indole aromatic moieties and alkynyl ligand (Fig. S1, ESI†). The low-energy, moderately intense absorption bands at 384–450 nm are attributed to the Pt(II)-perturbed IL_{Pt} N^C^N[π → π*] transition mixing with metal-to-ligand charge transfer (MLCT) [dπ(Pt) → π*(N^C^N)]. Due to the TSP, under 450 nm visible light (the IL and MLCT transition band) irradiation, the solution changed from colorless to bluish violet with the appearance of a new absorption band at 575 nm and gradually reaching the maximum on prolonged irradiation for 30 s (Fig. S2, ESI†). This phenomenon demonstrates that the TSP can cause visible light induced cleavage of the spiro C–O bond of **Pt-SP-Ph**, resulting in a π-conjugated **Pt-MC-Ph** isomer. This was further substantiated by ^{1}H NMR results, which revealed obvious changes in the proton signals relative to the **Pt-SP-Ph** isomer associated with the SP and Pt complex moieties (Fig. S3, ESI†). Subsequently, upon irradiation under 580 nm light, the **Pt-MC-Ph** isomer is converted back to the **Pt-SP-Ph** isomer with the observation of apparent color changes from bluish purple to colorless and the disappearance of the 575 nm absorption band. The photochromic process can be repeated for at least 8 cycles without obvious degradation, thanks to the intramolecular photosensitization reaction of the SP *via* the heavy-metal effect exerted by the Pt(II) center (Fig. S4, ESI†). As the rational design, the green emission band at 500 and 520 nm, originating from the Pt(II)-perturbed $^3IL_{Pt}$/^{3}MLCT [dπ(Pt) → π*(N^C^N)] excited state, shows good overlap with the absorption band of **Pt-MC-Ph**. Upon 450 nm visible-light irradiation, the TSP process is triggered. A new low-lying red emission at 642 nm, originating from the IL_{MC} [π → π*] excited state of enlarged π-conjugation MC moieties, appears and intensifies, accompanied by a decrease in the green light intensity (Fig. S5–S7, ESI†). This indicates that FRET is achieved due to the overlap of the wavelengths of absorption and emission, with an efficiency of *ca.* 20%. The assignments are further substantiated by the excitation spectra. The excitation spectra recorded at emission wavelengths of 620, 646, and 710 nm keep in line with the UV-vis spectrum, characteristic of the MC isomer, and differ from those obtained at 500, 530, and 580 nm, which correspond to the UV-vis spectrum of the SP isomer (Fig. S8, ESI†).

In order to explore **Pt-SP-Ph** as an optical information storage and anti-counterfeiting material, a thin film was firstly prepared by doping **Pt-SP-Ph** into poly(methyl methacrylate) (PMMA). The UV absorption and emission spectra of the film are similar to those in the solution state. Under 450 nm light illumination, the photochromic process occurs, and the apparent color changes from colorless to bluish purple, accompanied by a gradual change from the green emission to red (Fig. 1). Subsequently, the optical behaviors recover to the initial state upon 580 nm light irradiation. The reversible visible-light

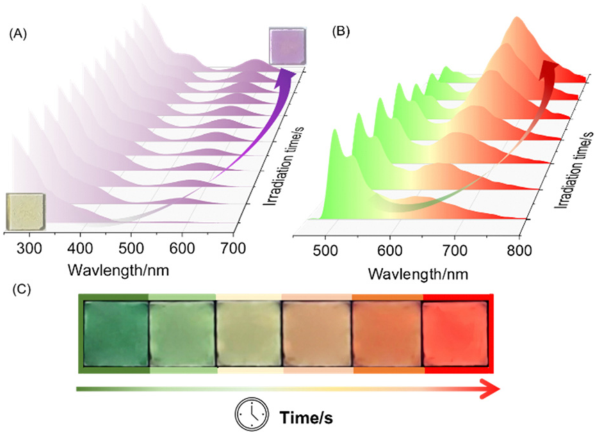

Fig. 1 Time-dependent (A) absorption and (B) emission spectra of **Pt-SP-Ph** upon 450 nm irradiation; (C) fluorescence color change of **Pt-SP-Ph** based on the synergism of photoisomerization and FRET with visible light irradiation time (λ_{ex} = 450 nm).

controlled photochromic conversion can be repeated at least 12 cycles, thanks to the TSP effect (Fig. S9, ESI†). Remarkably, the FRET efficiency (*ca.* 70%) is significantly improved compared to the solution state. The PMMA matrix offers a rigid space that stabilizes the MC isomer. This stabilization effect enhances the fluorescence resonance energy transfer from the donor to the acceptor. Moreover, the lifetime and quantum yield of the Pt(II) donor are improved, making the FRET process more competitive and further increasing the FRET efficiency (Fig. S10 and Table S1, ESI†).

Based on the excellent photochromic and FRET properties in the polymer film, we prepared a mixed solution of **Pt-SP-Ph** and PMMA to be used as an information storage and anti-counterfeiting material.

As shown in Fig. 2, a Koi carp image with a visual apparent purple color has been successfully patterned by exposing the substrate to the recording visible light (450 nm) by the mask method. The image can be erased by removing the mask and exposing to 450 nm light irradiation. The paper could be reused after 580 nm light irradiation.

As shown in Fig. 3, the information written using the PMMA inks containing different **Pt-SP-Ph** displays distinct apparent and emissive colors. Through the continuous irradiation of 450 nm visible light, the pattern of colorful auspicious clouds is observed. Under the irradiation of 580 nm light, the pattern disappears and the information is erased. The filter paper is soaked in a mixed solution of **Pt-SP-Ph** and PMMA and then cutted into a mushroom shape. By varying the visible light irradiation time, a mushroom pattern with the emission color varying continuously between green and red can be seen, showing good reversibility and tunability.

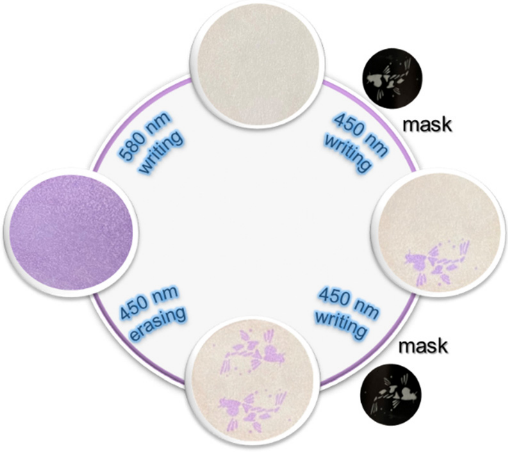

Fig. 2 Writing and erasing the Koi carp image with apparent color changes by the mask method on filter paper.

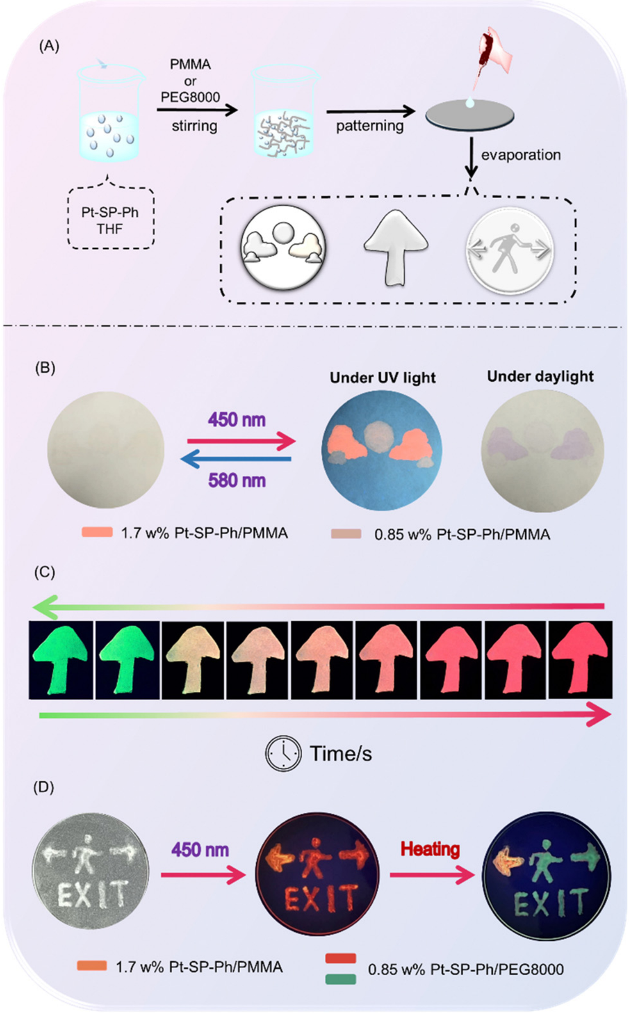

Fig. 3 (A) The description of the preparation of light-controlled dynamic patterns. (B) Apparent and luminescent photographs of colorful auspicious clouds prepared from **Pt-SP-Ph** doping with PMMA in different ratios. (C) Dynamic time-dependent luminescent photographs of mushroom patterns prepared from **Pt-SP-Ph** doping with PMMA. (D) Luminescent photographs of a safety exit indicator pattern prepared from **Pt-SP-Ph** doping with PMMA and PEG8000, respectively.

As we know, besides PMMA, polyethylene glycol (PEG) is also an excellent thermoplastic polymer with a low melting point. Herein, PMMA and PEG8000 were chosen for doping with **Pt-SP-Ph** as optical inks, respectively. A safety exit indicator pattern was drawn on a glass substrate using the two different polymer inks. Under continuous irradiation of visible light (450 nm), the whole pattern shows red emission in the form of **Pt-MC-Ph**, which means that both left and right are safe exit directions. In case of fire, as the temperature increases, the **Pt-MC-Ph/PEG8000** pattern displays rapid thermal bleaching to the **Pt-SP-Ph/PEG8000** form, resulting in green emission and the direction of the safety exit due to the FRET switching off. Meanwhile, the **Pt-MC-Ph/PMMA** pattern still shows red emission because of the slow isomerization and the FRET switching on. The distinct optical properties can be attributed to the excellent temperature response of PEG8000, which has a melting point of 64–66 °C and relatively low heat resistance. This characteristic provides a less rigid space and microenvironment that is conducive to the ring-closing reaction, requiring only a small activation energy. On the other hand, PMMA, with its higher melting point, offers advantages in high-temperature applications, as it has a glass transition temperature of approximately 105 °C.

In conclusion, a photo-controlled optical molecular switch containing the luminescent Pt(II) and photochromic SP functional moieties has been developed. Taking advantage of TSP characteristics, the fully visible light regulated photochromic process of the switch is realized with the improvement of fatigue resistance and stability (Table S2, ESI†). Meanwhile, efficient FRET can be conveniently regulated based on the controllable isomerization process in the film state. The photo- and temperature-responsive optical switch has been used to develop writing–erase information and anti-counterfeiting materials.

This work was supported by the National Natural Science Foundation of China (22201057 and 21871297), the Zhejiang Provincial Natural Science Foundation of China (LR22B010001 and LQ23B010001), and Hangzhou Normal University (2021 QDL001 and 2021QDL065).

Data availability

The data supporting this article have been included as part of the ESI.†

Conflicts of interest

There are no conflicts to declare.

Notes and references

1 N. Sinha, J. Wellauer, T. Maisuradze, A. Prescimone, S. Kupfer and O. S. Wenger, *J. Am. Chem. Soc.*, 2024, **146**, 10418–10431.
2 C. Zhao, Z. Ding, Y. Zhang, Z. Ni, S. Li, S. Gong, B. Zou, K. Wang and L. Yu, *Chem. Sci.*, 2023, **14**, 1089–1096.
3 W. Qi, C. Ma, P. Liao, H. Li, T. Gu, T. Wu, J. Huang and Y. Yan, *Adv. Opt. Mater.*, 2022, **11**, 2201229.
4 J. Wang, L. Zhang, W. Zhan, J. Dong, Y. Ma, J. Li, W. Li and C. Zhang, *Chem. Eng. J.*, 2024, **483**, 149078.
5 J. Volarić, W. Szymanski, N. A. Simeth and B. L. Feringa, *Chem. Soc. Rev.*, 2021, **50**, 12377–12449.
6 J. Peng, C. Han, X. Zhang, J. Jia, J. Bai, Q. Zhang, Y. Wang and P. Xue, *Angew. Chem., Int. Ed.*, 2023, **62**, e202311348.
7 J. Yang, X. Zhang, X. Zhang, L. Wang, W. Feng and Q. Li, *Adv. Mater.*, 2021, **33**, 2004754.
8 Y. Ma, J. Shen, J. Zhao, J. Li, S. Liu, C. Liu, J. Wei, S. Liu and Q. Zhao, *Angew. Chem., Int. Ed.*, 2022, e202202655.
9 W. A. Velema, J. P. van der Berg, M. J. Hansen, W. Szymanski, A. J. M. Driessen and B. L. Feringa, *Nat. Chem.*, 2013, **5**, 924–928.
10 W. Zhang, F. Huo, Y. Yue, Y. Zhang, J. Chao, F. Cheng and C. Yin, *J. Am. Chem. Soc.*, 2020, **142**, 3262–3268.
11 P. Hong, J. Liu, K.-X. Qin, R. Tian, L.-Y. Peng, Y.-S. Su, Z. Gan, X.-X. Yu, L. Ye, M.-Q. Zhu and C. Li, *Angew. Chem., Int. Ed.*, 2024, **63**, e202316706.
12 D. Kim, A. Aktalay, N. Jensen, K. Uno, M. L. Bossi, V. N. Belov and S. W. Hell, *J. Am. Chem. Soc.*, 2022, **144**, 14235–14247.
13 X. Feng, T. Wu, X. Sun and X. Qian, *J. Am. Chem. Soc.*, 2021, **143**, 21622–21629.
14 C. Xing, Z. Qi, B. Zhou, D. Yan and W.-H. Fang, *Angew. Chem., Int. Ed.*, 2024, **63**, e202402634.
15 Y.-J. Ma, X. Fang, G. Xiao and D. Yan, *Angew. Chem., Int. Ed.*, 2022, **61**, e202114100.
16 C. Xing, B. Zhou, D. Yan and W.-H. Fang, *CCS Chem.*, 2023, **5**, 2866–2876.
17 J.-X. Wang, C. Li and H. Tian, *Coord. Chem. Rev.*, 2021, **427**, 213579.
18 J. Zhang, S. Qin, S. Zhang, C. Sun, Y. Ren, L. Zhang, J. Liu, J. Xiao, W. Hu, H. Yang and D. Yang, *Adv. Mater.*, 2024, **36**, 2305872.
19 G. Das, T. Prakasam, N. Alkhatib, R. G. AbdulHalim, F. Chandra, S. K. Sharma, B. Garai, S. Varghese, M. A. Addicoat, F. Ravaux, R. Pasricha, R. Jagannathan, N. I. Saleh, S. Kirmizialtin, M. A. Olson and A. Trabolsi, *Nat. Commun.*, 2023, **14**, 3765.
20 X. Le, H. Shang, S. Wu, J. Zhang, M. Liu, Y. Zheng and T. Chen, *Adv. Funct. Mater.*, 2021, **31**, 2108365.
21 J. Kim, H. Yun, Y. J. Lee, J. Lee, S.-H. Kim, K. H. Ku and B. J. Kim, *J. Am. Chem. Soc.*, 2021, **143**, 13333–13341.
22 Y. Huang, H. K. Bisoyi, S. Huang, M. Wang, X.-M. Chen, Z. Liu, H. Yang and Q. Li, *Angew. Chem., Int. Ed.*, 2021, **60**, 11247–11251.
23 J. Guo, X. Wei, X. Fang, R. Shan and X. Zhang, *Sens. Actuators, B*, 2021, **347**, 130623.
24 I. F. Reis, F. B. Miguez, C. A. A. Vargas, T. G. Menzonatto, I. M. S. Silva, T. Verano-Braga, J. F. Lopes, T. A. S. Brandão and F. B. De Sousa, *ACS Appl. Mater. Interfaces*, 2020, **12**, 28607–28615.
25 Q. Qi, C. Li, X. Liu, S. Jiang, Z. Xu, R. Lee, M. Zhu, B. Xu and W. Tian, *J. Am. Chem. Soc.*, 2017, **139**, 16036–16039.
26 Y. Ai, Y. Fei, Z. Shu, Q. Zeng, Y. Zhang, Y. Zhu, X. Lei, J. Xu, J. Liu and Y. Li, *Adv. Opt. Mater.*, 2023, **11**, 2301047.
27 V. Guerchais, L. Ordronneau and H. Le Bozec, *Coord. Chem. Rev.*, 2010, **254**, 2533–2545.
28 Y. Li, A. Y.-Y. Tam, K. M.-C. Wong, W. Li, L. Wu and V. W.-W. Yam, *Chem. – Eur. J.*, 2011, **17**, 8048–8059.
29 V. W.-W. Yam, V. K.-M. Au and S. Y.-L. Leung, *Chem. Rev.*, 2015, **115**, 7589–7728.
30 M. Yoshida and M. Kato, *Coord. Chem. Rev.*, 2018, **355**, 101–115.
31 Y. Ai, Y. Li, M. H.-Y. Chan, G. Xiao, B. Zou and V. W.-W. Yam, *J. Am. Chem. Soc.*, 2021, **143**, 10659–10667.
32 Y. Wang, N. Li, L. Chu, Z. Hao, J. Chen, J. Huang, J. Yan, H. Bian, P. Duan, J. Liu and Y. Fang, *Angew. Chem., Int. Ed.*, 2024, **63**, e202403898.
33 S. Zhu, X. Lei, Q. Zeng, Y. Ai, X. Chen, Y. Lv, Y. Shao, G. Ji, T. Sun, G. Xiao and Y. Li, *Inorg. Chem. Front.*, 2024, **11**, 3992–4000.
34 A. M. Prokhorov, T. Hofbeck, R. Czerwieniec, A. F. Suleymanova, D. N. Kozhevnikov and H. Yersin, *J. Am. Chem. Soc.*, 2014, **136**, 9637–9642.
35 A. K. Chan, M. Ng, Y. C. Wong, M.-Y. Chan, W.-T. Wong and V. W.-W. Yam, *J. Am. Chem. Soc.*, 2017, **139**, 10750–10761.
36 J. Matern, I. Maisuls, C. A. Strassert and G. Fernández, *Angew. Chem., Int. Ed.*, 2022, **61**, e202208436.
37 J. Y.-W. Yeung, F. K.-W. Kong, F. K.-W. Hau, M. H.-Y. Chan, M. Ng, M.-Y. Leung and V. W.-W. Yam, *Angew. Chem., Int. Ed.*, 2022, **61**, e202207313.
38 F. K.-W. Kong, M.-C. Tang, Y.-C. Wong, M.-Y. Chan and V. W.-W. Yam, *J. Am. Chem. Soc.*, 2016, **138**, 6281–6291.
39 Q. Wan, K. Xiao, Z. Li, J. Yang, J. T. Kim, X. Cui and C.-M. Che, *Adv. Mater.*, 2022, **34**, 2204839.
40 Z. Wang, X. Jiang, K. Huang, L. Ning, J. Zhang, F. Zhang, J. Yang, Y. Wu, X. Chen, Y. Yi, X. Shi, Y. Chen and S. Wang, *Adv. Mater.*, 2021, **33**, 2106067.
41 X.-Q. Zhou, M. Mytiliniou, J. Hilgendorf, Y. Zeng, P. Papadopoulou, Y. Shao, M. P. Dominguez, L. Zhang, M. B. S. Hesselberth, E. Bos, M. A. Siegler, F. Buda, A. M. Brouwer, A. Kros, R. I. Koning, D. Heinrich and S. Bonnet, *Adv. Mater.*, 2021, **33**, 2008613.